

Phase diagram of non-Hermitian BCS superfluids in a dissipative asymmetric Hubbard model

Soma Takemori,* Kazuki Yamamoto, and Akihisa Koga

Department of Physics, Tokyo Institute of Technology, Meguro, Tokyo 152-8551, Japan

(Dated: November 27, 2024)

We investigate the non-Hermitian (NH) attractive Fermi-Hubbard model with asymmetric hopping and complex-valued interactions, which can be realized by collective one-body loss and two-body loss. By means of the NH BCS theory, we find that the weak asymmetry of the hopping does not affect the BCS superfluidity since it only affects the imaginary part of the eigenvalues of the BdG Hamiltonian. Systematic analysis in the d -dimensional hypercubic lattices clarifies that the singularity in the density of states affects the phase boundary between the normal and dissipation-induced superfluid states. Our results can be tested in ultracold atoms by using the photoassociation techniques and a nonlocal Rabi coupling with local losses and postselecting null measurement outcomes with the use of the quantum-gas microscope.

I. INTRODUCTION

Strongly correlated electron systems have attracted broad interest due to recent development of experimental techniques for ultracold atomic systems [1]. Due to the high controllability [2–7], the ultracold atomic systems can be regarded as the platform of quantum simulations [8–14]. In fact, many-body phenomena in the optical lattice have been realized such as in Mott insulating, antiferromagnetic, and superconducting states [15–19]. Recently, open systems, where the dissipation is inevitable due to the coupling to the environment, have attracted much attention [20–23]. This makes many-body physics more fruitful, and interesting phenomena have been observed such as dynamical sign reversal of the spin correlation [24] and the characteristic superfluid transport [25]. In addition, many experiments with dissipative process due to the inelastic collision of atoms have been conducted for, e.g., the single-body loss [25–34], the two-body loss [24, 35–40], and the three-body loss [41, 42]. These stimulate further theoretical investigations of the dissipation effect on the many-body physics [43–72].

The superfluid state in open systems has been widely investigated [73–87]. It has been clarified that, in addition to the conventional normal and superfluid states, the dissipation-induced (DS) superfluid state appears in the NH system, where the continuous quantum Zeno effect (QZE) induced by strong two-body losses plays an important role [76]. The effect of the asymmetric hopping, which can be realized by the nonlocal one-body loss, has been discussed so far. It has been clarified that fruitful phenomena are induced by nonreciprocal effects [88–92]. Then, a question arises; how stable is the superfluid state against both the nonlocal one-body loss and two-body loss in the ultracold fermionic systems?

To answer this question, we consider the NH attractive Hubbard model with complex-valued interactions and asymmetric hopping. To discuss how stable the superfluid state is against these dissipations, we employ the NH BCS theory and obtain the NH gap equation. Then, we clarify that the asymmetry of the hopping has no effects on the gap equation, and only contributes to the imaginary part of the dispersion rela-

tions. By performing the self-consistent calculations, we obtain the phase diagrams for the hypercubic lattice in arbitrary dimensions. In experiments, our model can be tested in ultracold atoms by postselecting the null measurement outcomes with the use of the quantum-gas microscope.

The rest of this paper is organized as follows. In Sec. II, we study the NH asymmetric Hubbard Hamiltonian with a complex-valued interaction on a cubic lattice. We clarify the effect of the asymmetric hopping on the BCS superfluidity in Sec. III. Section IV is devoted to the generalization of the results to arbitrary dimensions. Finally, a conclusion and discussion are given in Sec. V.

II. MODEL

We first consider the dissipative dynamics of ultracold fermionic atoms, which should be described by the following Markovian Lindblad equation [20]

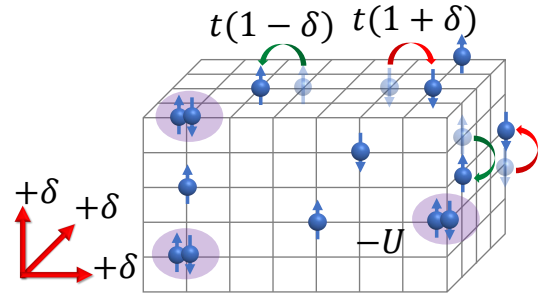


FIG. 1. Schematic image of the effective NH dynamics with asymmetric hopping and the complex-valued interactions due to the two-body losses on a three-dimensional optical lattice. The hopping amplitude t is modified with the asymmetry δ . Here, $t(1 \pm \delta)$ denotes the asymmetric hopping along the positive (negative) direction for x , y , and z axes (red and green arrows). The onsite interaction $U = U_1 + i\gamma/2$ has a complex value, where U_1 is the attractive interaction and γ is the rate of the two-body loss.

* s-takemori@stat.phys.titech.ac.jp

$$\frac{\partial \rho}{\partial t} = -i[H_0, \rho] + \mathcal{L}\rho, \quad (1)$$

$$\mathcal{L}\rho = \sum_i \mathcal{D}^{(i)}(\rho), \quad (2)$$

where ρ is the density matrix, H_0 is the Hamiltonian of the system, and

$$\mathcal{D}^{(i)}(\rho) = \sum_m L_m^{(i)} \rho L_m^{(i)\dagger} - (1/2)\{L_m^{(i)\dagger} L_m^{(i)}, \rho\}, \quad (3)$$

is the dissipator for the Lindblad operator $L_m^{(i)}$. When two-component fermionic atoms in a three-dimensional optical lattice are considered, the Hamiltonian H_0 is given as

$$H_0 = -t \sum_{\langle i,j \rangle, \sigma} (c_{i,\sigma}^\dagger c_{j,\sigma} + \text{H.c.}) - \mu \sum_{i,\sigma} n_{i,\sigma} - U \sum_i c_{i,\uparrow}^\dagger c_{i,\downarrow}^\dagger c_{i,\downarrow} c_{i,\uparrow}, \quad (4)$$

where $c_{i,\sigma} (c_{i,\sigma}^\dagger)$ is the annihilation (creation) operator of a fermion with spin $\sigma (= \uparrow, \downarrow)$ at site i , $\langle i, j \rangle$ means the summation over nearest neighbor pairs that satisfies $i < j$, and $n_{i,\sigma} (= c_{i,\sigma}^\dagger c_{i,\sigma})$ is the particle number operator, t is the hopping amplitude, μ is the chemical potential, and U_1 is the attractive interaction.

In this study, we consider the collective one-body loss and two-body loss as dissipation in the ultracold atomic systems. The Lindblad operator for the collective one-body loss is given by $L_{i,j,\sigma}^{(1)} = \sqrt{\gamma_1}(c_{i,\sigma} + i c_{j,\sigma})$ with the rate γ_1 . $L_i^{(2)} = \sqrt{\gamma_2} c_{i,\downarrow} c_{i,\uparrow}$ describes the two-body loss at site i with rate γ_2 . The collective one-body loss is realized through a nonlocal Rabi coupling between the lattice and an additional auxiliary lattice [79, 92–94]. The details are provided explicitly in Appendix A. The dissipative dynamics is then described as

$$\frac{\partial \rho}{\partial t} = -i(H_{\text{eff}}\rho - \rho H_{\text{eff}}^\dagger) + \sum_{\langle i,j \rangle, \sigma} L_{i,j,\sigma}^{(1)} \rho L_{i,j,\sigma}^{(1)\dagger} + \sum_i L_i^{(2)} \rho L_i^{(2)\dagger}, \quad (5)$$

where the effective Hamiltonian is given as,

$$H_{\text{eff}} = -t \sum_{\langle i,j \rangle, \sigma} [(1 + \delta) c_{i,\sigma}^\dagger c_{j,\sigma} + (1 - \delta) c_{j,\sigma}^\dagger c_{i,\sigma}] - \mu \sum_{i,\sigma} n_{i,\sigma} - U \sum_i c_{i,\uparrow}^\dagger c_{i,\downarrow}^\dagger c_{i,\downarrow} c_{i,\uparrow}, \quad (6)$$

where $\delta = \gamma_1/(2t)$, $\gamma = \gamma_2$, and $U (= U_1 + i\gamma/2)$ is the complex-valued interaction. We have ignored the term $-i\delta \sum_{i,\sigma} n_{i,\sigma}$ since it does not affect the results qualitatively. The nonlocal one-body loss and two-body loss lead to the direction-dependent hopping and complex-valued interactions in the effective NH Hamiltonian H_{eff} , respectively. The effective NH Hamiltonian is schematically shown in Fig. 1.

To extract the effective dynamics of the NH Hamiltonian (6), we employ the quantum trajectory method [20],

which is obtained by stochastically unraveling the Lindblad equation (5). The quantum trajectory is characterized by two parts: the nonunitary Schrödinger evolution process under the NH Hamiltonian (6), and the quantum-jump process described by the Lindblad operator in the last two terms of Eq. (5). By postselecting the special measurement outcomes where the quantum jump does not occur, the effective dynamics of the system is described by the NH Hamiltonian (6).

By using the Fourier transformation

$$c_{i,\sigma} = \sqrt{\frac{1}{N}} \sum_{\mathbf{k}} c_{\mathbf{k},\sigma} e^{i\mathbf{k} \cdot \mathbf{r}_i}, \quad (7)$$

the effective Hamiltonian reads

$$H_{\text{eff}} = \sum_{\mathbf{k}, \sigma} \xi_{\mathbf{k}} c_{\mathbf{k},\sigma}^\dagger c_{\mathbf{k},\sigma} - \frac{U}{N} \sum_{\mathbf{k}, \mathbf{k}'} c_{\mathbf{k},\uparrow}^\dagger c_{-\mathbf{k},\downarrow}^\dagger c_{-\mathbf{k}',\downarrow} c_{\mathbf{k}',\uparrow}, \quad (8)$$

$$\xi_{\mathbf{k}} = -2t \sum_{j=x,y,z} \cos k_j - 2it\delta \sum_{j=x,y,z} \sin k_j - \mu, \quad (9)$$

where N is the number of the sites. We find that two kinds of dissipation make the Hamiltonian non-Hermitian, that is, the collective one-body loss yields the imaginary part of the dispersion relations and the two-body loss yields the imaginary part of the interactions.

III. NH BCS THEORY WITH ASYMMETRIC HOPPING AND A COMPLEX-VALUED INTERACTION AND THE EFFECT OF THE ASYMMETRY OF THE HOPPING

Here, we deal with the NH Hamiltonian (8) in the framework of the NH BCS theory [76]. The NH BCS mean-field Hamiltonian is given by

$$H_{\text{eff}}^{\text{BCS}} = \sum_{\mathbf{k}} \mathbf{v}_{\mathbf{k}}^\dagger \hat{M}_{\mathbf{k}} \mathbf{v}_{\mathbf{k}} + E_0, \quad (10)$$

$$\hat{M}_{\mathbf{k}} = \begin{pmatrix} \xi_{\mathbf{k}} & \Delta \\ \bar{\Delta} & -\xi_{\mathbf{k}}^* \end{pmatrix}, \quad (11)$$

where $\mathbf{v}_{\mathbf{k}}^\dagger = (c_{\mathbf{k},\uparrow}^\dagger, c_{-\mathbf{k},\downarrow}^\dagger)$, Δ and $\bar{\Delta}$ are the superfluid order parameters, and $E_0 = N\Delta\bar{\Delta}/U + \sum_{\mathbf{k}} \xi_{\mathbf{k}}^*$. To evaluate the superfluid order parameter, we define the right (left) BCS state $|\text{BCS}\rangle_{R(L)}$ as a vacuum state of Bogoliubov quasiparticle operators as follows:

$$|\text{BCS}\rangle_R = \prod_{\mathbf{k}} (u_{\mathbf{k}} + v_{\mathbf{k}} c_{\mathbf{k},\uparrow}^\dagger c_{-\mathbf{k},\downarrow}^\dagger) |0\rangle, \quad (12)$$

$$|\text{BCS}\rangle_L = \prod_{\mathbf{k}} (u_{\mathbf{k}}^* + \bar{v}_{\mathbf{k}} c_{\mathbf{k},\uparrow}^\dagger c_{-\mathbf{k},\downarrow}^\dagger) |0\rangle, \quad (13)$$

where $u_{\mathbf{k}}, v_{\mathbf{k}}, \bar{v}_{\mathbf{k}}$ are the coefficients and $|0\rangle$ is the vacuum for the fermion. Then, the superfluid order parameters are given by

$$\Delta = -\frac{U}{N} \sum_{\mathbf{k}} L \langle c_{-\mathbf{k},\downarrow} c_{\mathbf{k},\uparrow} \rangle_R, \quad (14)$$

$$\bar{\Delta} = -\frac{U}{N} \sum_{\mathbf{k}} L \langle c_{\mathbf{k},\uparrow}^\dagger c_{-\mathbf{k},\downarrow}^\dagger \rangle_R, \quad (15)$$

where we have introduced the NH expectation value as ${}_L\langle \cdot \rangle_R \equiv {}_L\langle \text{BCS} | \cdot | \text{BCS} \rangle_R$. We note that these order parameters (14) and (15) are complex in general. Since the energy dispersion (9) satisfies $\text{Re}\xi_{\mathbf{k}} = \text{Re}\xi_{-\mathbf{k}}$ and $\text{Im}\xi_{\mathbf{k}} = -\text{Im}\xi_{-\mathbf{k}}$, the matrix $\hat{M}_{\mathbf{k}}$ can be divided into two terms as

$$\hat{M}_{\mathbf{k}} = \begin{pmatrix} \text{Re}\xi_{\mathbf{k}} & \Delta \\ \bar{\Delta} & -\text{Re}\xi_{\mathbf{k}} \end{pmatrix} + i\text{Im}\xi_{\mathbf{k}}\hat{I}, \quad (16)$$

where \hat{I} is the identity matrix. We note that the imaginary part of the dispersion relation has no effects on the Bogoliubov transformation since the latter term is represented by the identity matrix. Then, this simply affects the imaginary part of the dispersion for the quasiparticles. This is in contrast to the Zeeman effects in the BCS theory, the transformation of which is represented by the identity matrix with a real coefficient. It is known that the magnetic field affects the dispersion relation for the quasiparticles and the superconducting state becomes unstable [95–97].

One can diagonalize the Hamiltonian (10) as

$$H_{\text{eff}}^{\text{BCS}} = \sum_{\mathbf{k}} [E_{\mathbf{k},+}\bar{\gamma}_{\mathbf{k},\uparrow}\gamma_{\mathbf{k},\uparrow} + E_{\mathbf{k},-}\bar{\gamma}_{-\mathbf{k},\downarrow}\gamma_{-\mathbf{k},\downarrow}] + E_g, \quad (17)$$

with

$$E_{\mathbf{k},\pm} = \tilde{\epsilon}_{\mathbf{k}} \pm i\text{Im}\xi_{\mathbf{k}}, \quad (18)$$

$$E_g = E_0 - \sum_{\mathbf{k}} E_{\mathbf{k},-}, \quad (19)$$

where $\tilde{\epsilon}_{\mathbf{k}} = \sqrt{(\text{Re}\xi_{\mathbf{k}})^2 + \Delta\bar{\Delta}}$. The quasiparticle operators are calculated by using the Bogoliubov transformations as

$$\bar{\gamma}_{\mathbf{k},\uparrow} = u_{\mathbf{k}}c_{\mathbf{k},\uparrow}^\dagger - \bar{v}_{\mathbf{k}}c_{-\mathbf{k},\downarrow}, \quad (20)$$

$$\gamma_{-\mathbf{k},\downarrow} = v_{\mathbf{k}}c_{\mathbf{k},\uparrow}^\dagger + u_{\mathbf{k}}c_{-\mathbf{k},\downarrow}, \quad (21)$$

$$\gamma_{\mathbf{k},\uparrow} = u_{\mathbf{k}}c_{\mathbf{k},\uparrow} - v_{\mathbf{k}}c_{-\mathbf{k},\downarrow}^\dagger, \quad (22)$$

$$\bar{\gamma}_{-\mathbf{k},\downarrow} = \bar{v}_{\mathbf{k}}c_{\mathbf{k},\uparrow} + u_{\mathbf{k}}c_{-\mathbf{k},\downarrow}^\dagger, \quad (23)$$

with the coefficients

$$u_{\mathbf{k}} = \sqrt{\frac{\tilde{\epsilon}_{\mathbf{k}} + \text{Re}\xi_{\mathbf{k}}}{2\tilde{\epsilon}_{\mathbf{k}}}}, \quad (24)$$

$$v_{\mathbf{k}} = -\sqrt{\frac{\tilde{\epsilon}_{\mathbf{k}} - \text{Re}\xi_{\mathbf{k}}}{2\tilde{\epsilon}_{\mathbf{k}}}} \frac{\sqrt{\Delta}}{\sqrt{\bar{\Delta}}}, \quad (25)$$

$$\bar{v}_{\mathbf{k}} = -\sqrt{\frac{\tilde{\epsilon}_{\mathbf{k}} - \text{Re}\xi_{\mathbf{k}}}{2\tilde{\epsilon}_{\mathbf{k}}}} \frac{\sqrt{\Delta}}{\sqrt{\bar{\Delta}}}, \quad (26)$$

where $u_{\mathbf{k}}^2 + v_{\mathbf{k}}\bar{v}_{\mathbf{k}} = 1$. Although $\bar{\gamma}_{\mathbf{k},\sigma}$ is not the Hermitian conjugate of $\gamma_{\mathbf{k},\sigma}$ due to the complexity of Δ and $\bar{\Delta}$, the quasiparticle operators satisfy the anticommutation relations $\{\bar{\gamma}_{\mathbf{k},\sigma}, \gamma_{\mathbf{k}',\sigma'}\} = \delta_{\mathbf{k},\mathbf{k}'}\delta_{\sigma,\sigma'}$. The BCS states (12) and (13) satisfy $\gamma_{\mathbf{k},\sigma}|\text{BCS}\rangle_R = 0$ and $\bar{\gamma}_{\mathbf{k},\sigma}^\dagger|\text{BCS}\rangle_L = 0$. In the end, we obtain the NH gap equation as

$$\frac{1}{U} = \frac{1}{N} \sum_{\mathbf{k}} \frac{1}{2\tilde{\epsilon}_{\mathbf{k}}} = \int d\epsilon \frac{D(\epsilon)}{2\sqrt{\epsilon^2 + \Delta_0^2}}, \quad (27)$$

where the effective density of states (DOS) is defined as

$$D(\epsilon) = \frac{1}{N} \sum_{\mathbf{k}} \delta(\epsilon - \text{Re}\xi_{\mathbf{k}}), \quad (28)$$

where $\delta(x)$ is the delta function. We note that the DOS is given only by the real part of the dispersion relations and the imaginary part does not appear in Eq. (28). This means that the DOS is not affected by the asymmetry of the hopping.

The gap equation (27) is different from that in the Hermitian system since U and $\Delta\bar{\Delta}$ are complex values. Hereafter, we take the special gauge $\Delta_0 = \Delta = \bar{\Delta}$ without loss of generality. In this case, the order parameter Δ_0 is complex and smoothly approaches the real value with $\gamma \rightarrow 0$. To study the stability of the superfluid state against dissipation, we calculate the condensation energy as

$$\begin{aligned} \frac{E_{\text{cond}}}{N} &= \frac{E_g - E_N}{N} \\ &= \frac{\Delta_0^2}{U} - \int d\epsilon D(\epsilon) \left(\sqrt{\epsilon^2 + \Delta_0^2} - |\epsilon| \right), \end{aligned} \quad (29)$$

where E_N is the energy for the normal state. We use the real part of the condensation energy (29) to discuss the stability of the superfluid state. The average of the filling is given by

$$n = \frac{1}{N} \sum_{\mathbf{k},\sigma} {}_L\langle c_{\mathbf{k},\sigma}^\dagger c_{\mathbf{k},\sigma} \rangle_R \quad (30)$$

$$= \int d\epsilon D(\epsilon) \left(1 - \frac{\epsilon}{\sqrt{\epsilon^2 + \Delta_0^2}} \right). \quad (31)$$

When $\mu = 0$, we get $n = 1$. As the number-preserving state is realized in realistic systems, the expectation value of the total particle number $\sum_{\mathbf{k},\sigma} {}_L\langle c_{\mathbf{k},\sigma}^\dagger c_{\mathbf{k},\sigma} \rangle_R$ is conserved and gives a real number. Hereafter, we set $\mu = 0$.

We note that the effect of the asymmetric hopping δ does not appear in the effective DOS (28), the NH gap equation (27), and the condensation energy (29). This means that the asymmetric hopping has no effect on the superfluidity within the mean-field approximation. In particular, when $\gamma = 0$, the conventional superfluid state with a finite order parameter is stable against the asymmetric hopping within the mean-field approximation although its lifetime should be finite. By contrast, the quasiparticle energy $E_{\mathbf{k}}$ depends on δ . Here, we show in Fig. 2 the real and imaginary parts of the quasiparticle energy $E_{\mathbf{k}}$ in the system with $U_1/t = 3$ and $\gamma/t = 1$ when $\delta = 0$ and 0.1. The real part of the quasiparticle energy is regarded as the effective energy of quasiparticles and the imaginary part of that is regarded as the lifetime of quasiparticles. When we increase δ , the real part of the quasiparticle energy never changes, while the imaginary part is induced with changing the sign in reciprocal space, as shown in Fig. 2(c). This means that the lifetime of the quasiparticles on particular regions is amplified. If the asymmetric hopping is considered in the Hamiltonian as $H = -t \sum_{\langle i,j \rangle, \sigma} (e^\alpha c_{i,\sigma}^\dagger c_{j,\sigma} + e^{-\alpha} c_{j,\sigma}^\dagger c_{i,\sigma})$, both t and δ in our Hamiltonian (6) are formally changed. However, by rescaling the energy unit, we obtain the simple phase diagram, which will be discussed in Appendix B.

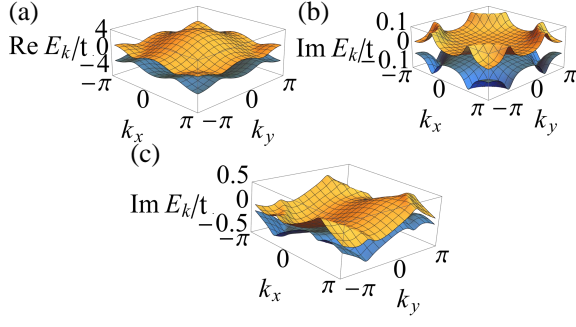


FIG. 2. (a) The real part and (b) the imaginary part of the quasiparticle energy $E_{\mathbf{k}} = E_{\mathbf{k},+}, -E_{\mathbf{k},-}$ (orange for the positive sign and blue for the negative sign) when $\delta = 0$. (c) The imaginary part of the $E_{\mathbf{k}}$ when $\delta = 0.1$. Dispersion relations with $k_z = 0$ for quasiparticles in the system with $U_1/t = 3$ and $\gamma/t = 1$ are used.

IV. GENERALIZATION TO ARBITRARY DIMENSIONS

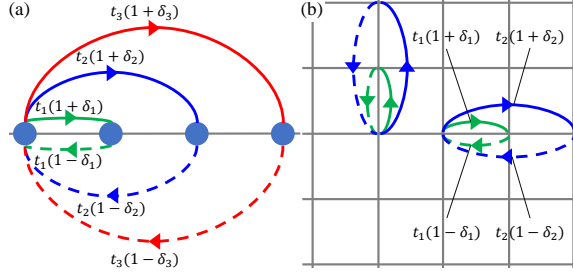


FIG. 3. Schematic image of the asymmetric hopping in the d -dimensional hypercubic lattice when (a) $d = 1$ and (b) $d = 2$. We consider the hopping across several lattice sites in the same direction, for example, the hopping amplitude between nearest neighbor sites is $t_1(1 \pm \delta_1)$, the hopping between next-nearest neighbor sites is $t_2(1 \pm \delta_2)$, and the hopping between m -th nearest neighbor sites is $t_m(1 \pm \delta_m)$.

In this section, we consider a d -dimensional NH Hubbard model with asymmetric hopping and complex-valued interactions. For the sake of simplicity, we consider a hypercubic lattice. The Hamiltonian is given by

$$H_{\text{eff}} = H_{\text{kin}} + H_{\text{int}}, \quad (32)$$

$$H_{\text{kin}} = - \sum_m t_m \sum_{\langle i,j \rangle_{m,\sigma}} \left[(1 + \delta_m) c_{i,\sigma}^\dagger c_{j,\sigma} + (1 - \delta_m) c_{j,\sigma}^\dagger c_{i,\sigma} \right], \quad (33)$$

$$H_{\text{int}} = -U \sum_i c_{i,\uparrow}^\dagger c_{i,\downarrow}^\dagger c_{i,\downarrow} c_{i,\uparrow}, \quad (34)$$

where t_m is the hopping to the m -th nearest neighbor sites in the same direction, $\langle i,j \rangle_m$ means the summation over the m -th nearest neighbor pairs, and δ_m is its asymmetry. In our discussions, we only consider the hopping across lattice sites in the same direction (see Fig. 3), which is regarded as the generalization of the Hatano-Nelson model [89–91]. In the

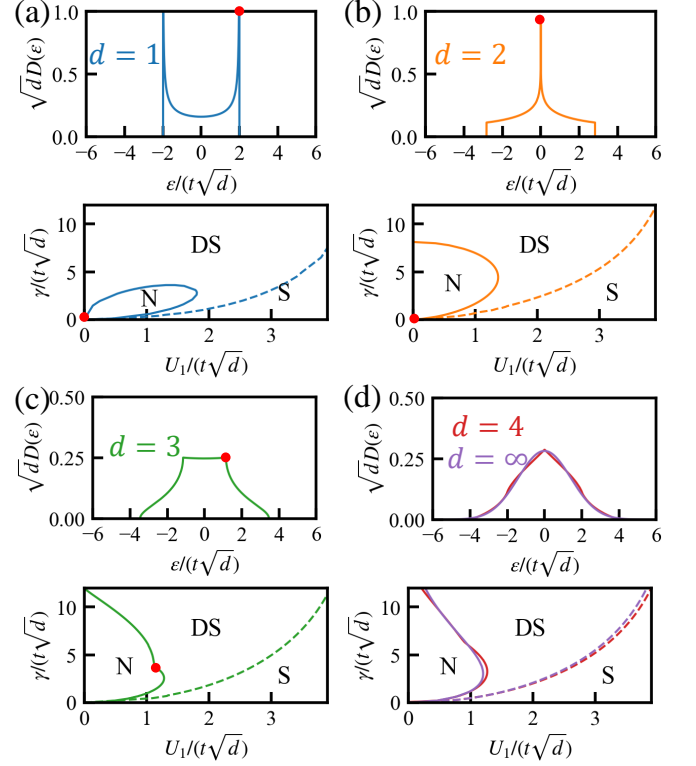


FIG. 4. The DOS and the phase diagram of the d -dimensional attractive Hubbard model with two-body loss and asymmetric nearest neighbor hopping when (a) $d = 1$, (b) $d = 2$, (c) $d = 3$, and (d) $d = 4, \infty$. N, DS, and S denote the normal state, the DS state, and the superfluid state, respectively. The hopping amplitude is rescaled as $t\sqrt{d}$ based on the energy unit on an infinite dimensional system [98, 99]. The red point denotes the singular point in DOS in upper figures, and it affects the phase boundary in lower figures.

noninteracting case, the dispersion relation is given as

$$\xi_{\mathbf{k}} = - \sum_m \sum_{l=1}^d \left[2t_m \cos(mk_l) + 2it_m \delta_m \sin(mk_l) \right]. \quad (35)$$

The long-range hopping and dimensionality in the system can be captured in Eq. (35), and the asymmetric effect only appears in its imaginary part. This property is essentially the same as the simpler case discussed above. Therefore, no effect of the asymmetric hopping appears, as far as we consider the generalized model (32) in the framework of the BCS theory.

Figure 4 shows the DOS and the phase diagram on the d -dimensional NH Hubbard model with nearest-neighbor hopping. The normal (N) state is characterized by a trivial solution of the NH gap equation (27), and the superfluid (S) and the dissipation-induced superfluid (DS) states are characterized by the nontrivial solution. In the S (DS) state, the real part of the condensation energy is $\text{Re}E_{\text{cond}} < 0 (> 0)$. We find that, in the phase diagram, the N state appears in the small U and intermediate dissipation rate γ , the ordered state with finite Δ_0 is widely realized for any dimensions.

One of the important features inherent in the NH system

is the emergence of the exceptional points (EPs). When the system crosses the phase boundary from the DS state to the N state, the real part of the order parameter gradually approaches to zero, while the imaginary part suddenly vanishes from ϵ_0 which satisfies $\epsilon_0 = \pm \text{Im}\Delta_0/t$. When the transition occurs, the effective Hamiltonian cannot be diagonalized, and EPs emerge in the reciprocal space. This is equivalent to the divergence of the integral function at $\epsilon = \epsilon_0$ in the gap equation (27). Importantly, this means that EPs as well as DOS play a crucial role in the NH gap equation [85]. Namely, the DS state is expanded due to the large DOS at $\epsilon = \epsilon_0$. In one dimensions, the N state is surrounded by the DS state in the phase diagram, which is shown in Fig. 4(a). The corresponding phase boundary strongly reflects the singularity in the DOS at $\epsilon/t = \pm 2$. This behavior is characteristic of one dimensions. In two dimensions, DOS has a singularity at $\epsilon = 0$. However, this little affects the phase diagram since the corresponding phase boundary is located at the origin of the diagram, as shown in Fig. 4(b). The DOS in three dimensions has the cusp singularity at $\epsilon/t = 2$, leading to the small cusp singularity in the phase boundary at $(U_1/t, \gamma/t) \sim (1.9, 6.5)$. In larger dimensions, the singularity in the DOS tends to smear, and no singularity appears in the hypercubic lattice with $d \rightarrow \infty$.

These results indicate that the reentrant superfluidity for small U_1 with increasing dissipation is ubiquitous for any dimensional hypercubic lattices. Such a unique phase boundary can be detected by using the photoassociation techniques [40] and postselecting the null measurement outcomes with the use of the quantum-gas microscope [43, 100–104].

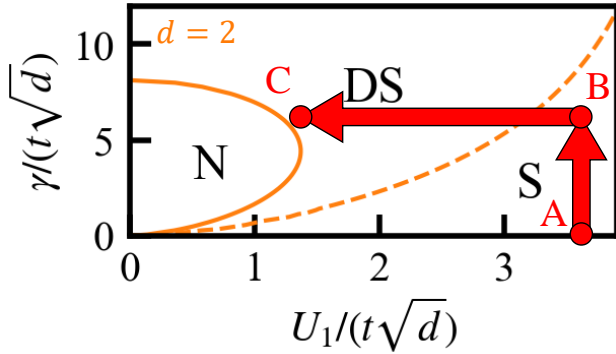


FIG. 5. Experimental protocol to reach the dissipation-induced superfluid for strong dissipation. Here, we use the phase diagram for the square lattice and the same protocol can be done in the other dimensions. First, we prepare a superfluid state for large attraction U_1 (A) and then introduce large dissipation γ by utilizing a photoassociation technique (B). Finally, the system will reach the dissipation-induced superfluid regime by decreasing U_1 (C).

V. CONCLUSIONS AND DISCUSSIONS

In this paper, we have considered the three-dimensional attractive Hubbard model with fundamental dissipation, i.e., asymmetric hopping and complex-valued interactions which

can be realized by the collective one-body loss and two-body loss in the ultracold fermionic systems. We have demonstrated that the asymmetry of the hopping has no effects on the fermionic superfluidity within the NH BCS approximation. It has been found that the complex-valued interactions yield the reentrant phase transitions, as discussed in the previous works. In particular, we have confirmed that the singularity of the noninteracting DOS leads to the singularity in the phase boundary between the dissipation-induced superfluid and normal states.

Our system can be implemented in ultracold atoms [76]. We can use, e.g., ^6Li , ^{40}K and ^{173}Yb in an optical lattice with attractive interaction, two-body loss, and asymmetric hopping. The hopping amplitude t can be changed by tuning the lattice depth. By using the Feshbach resonance, we can control the attractive interaction U_1 [3]. The asymmetric hopping can be realized by means of the nonlocal Rabi coupling [79, 92, 94] and two-body loss can be realized by using the photoassociation [24, 38]. For the detailed discussion, we refer the reader to Appendix A. The NH phase for strong dissipation can be accessed in experiments by using the QZE. As the timescale of quantum jumps is estimated as $1/\gamma$ and the relaxation timescale towards the quasiequilibrium state is given by $1/t$, the energy scale of γ and t should be comparable to realize the NH dynamics. In Fig. 5, we illustrate the experimental protocol for reaching the NH phase in the strong dissipation regime that satisfies $\gamma/t \sim 5$. We first prepare a superfluid for large attraction U_1 [(A) in Fig. 5] and increase the two-body loss rate [(B) in Fig. 5] by using photoassociation techniques [24, 38]. Finally, we ramp down the attraction U_1 with the use of the Feshbach resonance [(C) in Fig. 5]. If we do not have dissipation, atoms that form the on-site molecular pairs tunnel to neighboring sites at a timescale $1/t$. However, under strong dissipation, the hopping of the atoms to the neighbor sites are suppressed due to QZE and the atoms are tightly coupled to form on-site molecules. Then, we can see the delay of dissociation of such QZE-assisted molecules even after a timescale $1/t$, and this can be a signature of the dissipation-induced superfluid.

Although we consider the hypercubic lattice, it is interesting to explore the NH quantum phase transition of the dissipative Hubbard model with asymmetric hopping on a bipartite lattice. The asymmetric hopping in NH systems will play a crucial role in studying the symmetry and topological classification [92, 105, 106]. Then, exploring the topological phase transition in the NH Hubbard model with asymmetric hopping may be a novel research. Furthermore, investigating the attractive NH Hubbard model on the one-dimensional system with multiple dissipation with the use of a more precise method, such as the Bethe ansatz [59, 88], remains future work. Analysis of the Lindblad dynamics with asymmetric hopping and two-body loss is another important pursuit. We hope that this paper contributes to the understanding of the NH system with fundamental dissipation. In the view of quantum trajectory approach [20], the NH system describes the special case of the dynamics of the quantum trajectory which represents the measurement-induced phase transition [107–115]. More recently, as the dissipative system with gain has been re-

alized in ultracold atoms [116], the study of the NH fermionic superfluidity with gain and loss is also interesting. Exploring the NH many-body physics can give a fundamental concept of open quantum systems.

ACKNOWLEDGMENTS

We would like to thank Hiroyuki Tajima and Masaya Nakagawa for fruitful discussions. This work was supported by Grant-in-Aid for Scientific Research from JSPS, KAKENHI Grants No. JP23K19031 (K.Y.), and No. JP22K03525 (A.K.). K.Y. was also supported by Yamaguchi Educational and Scholarship Foundation, Toyota RIKEN Scholar program, Murata Science and Education Foundation, and Public Promoting Association Kura Foundation.

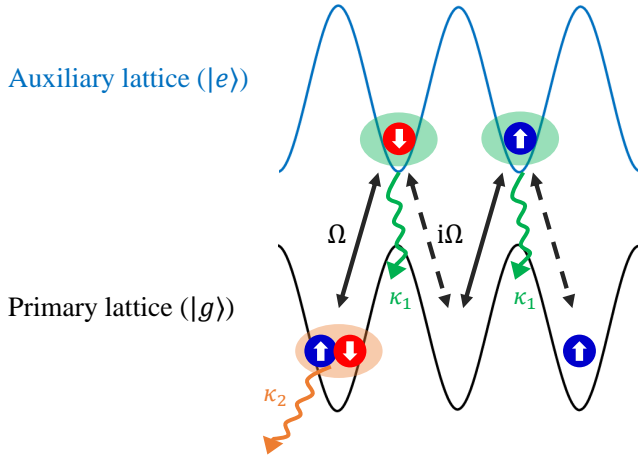


FIG. 6. Schematic image of our system. We consider the dissipative dynamics of fermionic atoms in primary (Black) and auxiliary (Blue) lattices. The Rabi coupling between the primary and auxiliary lattices is introduced by using a running wave [92] and the rate is changed by i compared with the left nearest sites. We introduce the one-body loss with rate κ_1 to the auxiliary lattice and the two-body loss with rate κ_2 to the primary lattice.

Appendix A: Experimental setup for realizing our system

In this section, we briefly explain how the asymmetric hopping can be realized in experiments, following the paper [92]. We start from the ultracold fermionic atoms in an optical lattice with an auxiliary lattice, where the potential minima of the auxiliary lattice are positioned at the middles for that of the primary lattice, as shown in Fig. 6. For the sake of simplicity, we treat with a one-dimensional system, and extension for higher dimensions will follow similarly. The full dynamics is described by the following Markovian Lindblad equation [20]

$$\frac{\partial \rho}{\partial t} = -i[H_0 + V, \rho] + \mathcal{D}[\tilde{L}_{i,\sigma}^{(1)}]\rho + \mathcal{D}[\tilde{L}_i^{(2)}]\rho, \quad (\text{A1})$$

where ρ is the density matrix. Here, the Hermitian Hamiltonian $H = H_g + H_e + V$ is written as

$$H_g = -t \sum_{\langle i,j \rangle, \sigma} (c_{i,\sigma,g}^\dagger c_{j,\sigma,g} + \text{H.c.}) - \mu \sum_{i,\sigma} n_{i,\sigma,g} - U_1 \sum_i c_{i,\uparrow,g}^\dagger c_{i,\downarrow,g}^\dagger c_{i,\downarrow,g} c_{i,\uparrow,g}, \quad (\text{A2})$$

$$H_e = -t \sum_{\langle i,j \rangle, \sigma} (c_{i,\sigma,e}^\dagger c_{j,\sigma,e} + \text{H.c.}) - \mu \sum_{i,\sigma} n_{i,\sigma,e}, \quad (\text{A3})$$

$$V = \frac{\Omega}{2} \sum_{i,\sigma} [c_{i,\sigma,e}^\dagger (c_{i,\sigma,g} + i c_{i+1,\sigma,g}) + \text{H.c.}], \quad (\text{A4})$$

where $c_{i,\sigma,\alpha}$ ($c_{i,\sigma,\alpha}^\dagger$) is the annihilation (creation) operator of the fermion with spin $\sigma = \uparrow, \downarrow$ at site i . The primary (auxiliary) lattice is denoted as $\alpha = g(e)$ and the coupling strength between the primary and auxiliary lattices is introduced as Ω . To describe the dissipation, we introduce the Lindblad operator \tilde{L}_m that describes the dissipative event at characteristic rates. The one-body loss of the auxiliary lattice is described by $\tilde{L}_{i,\sigma}^{(1)} = \sqrt{\kappa_1} c_{i,\sigma,e}$ where κ_1 is the dissipation rate. The operator $\tilde{L}_i^{(2)} = \sqrt{\kappa_2} c_{i,\downarrow,g} c_{i,\uparrow,g}$ describes the two-body loss of the primary lattice at site i at a rate κ_2 , which generates the complex-valued interaction.

To extract the effective dynamics of the primary lattice, we employ the adiabatically elimination [79, 92–94], which changes the local loss of the auxiliary lattice into the nonlocal loss of the primary lattice. Then, in the regime where $\kappa_1 \gg \Omega$, the Lindblad equation which describes the effective dynamics of the primary lattice is written as

$$\frac{\partial \rho}{\partial t} = -i[H_g, \rho] + \mathcal{D}[L_{\text{eff},i,\sigma}^{(1)}]\rho + \mathcal{D}[L_{\text{eff},i}^{(2)}]\rho. \quad (\text{A5})$$

The effective Lindblad operator $L_{\text{eff},i,\sigma}^{(1)}, L_{\text{eff},i}^{(2)}$ are the same as in Eq. (5), where the parameters are related to each other by

$$\gamma_1 = \Omega^2 / \kappa_1, \quad \gamma_2 = \kappa_2. \quad (\text{A6})$$

Then, by focusing on the effective short-time dynamics that is described by the NH Hamiltonian obtained from Eq. (A5), we arrive at Eq. (6) in Sec. II.

Here, we present the detailed values of experimental parameters by using ^{173}Yb as an example. First, the hopping amplitude t can be changed by tuning the lattice depth. By using the Feshbach resonance, we can control the attractive interaction U_1 . In Ref. [24], the hopping amplitude and repulsive interaction strength are estimated to be several kHz for the repulsive Fermi Hubbard model on the dimerized lattice. By tuning the magnetic field strength, we can change the interaction strength to be negative. Second, we can control the one-body loss rate κ_1 in the auxiliary lattice and the asymmetry of the hopping δ by tuning the Rabi coupling Ω between the primary and auxiliary lattices. The coupling constant between two hyperfine state is estimated to be several kHz [34]. The one-body loss can be introduced by using a near-resonant optical beam, e.g., the loss rate $\kappa_1 \sim \text{kHz}$ is used with ^6Li in Ref. [30]. Similar protocols will follow in ^{173}Yb and it is necessary to enhance the loss rate by employing a high power beam to realize

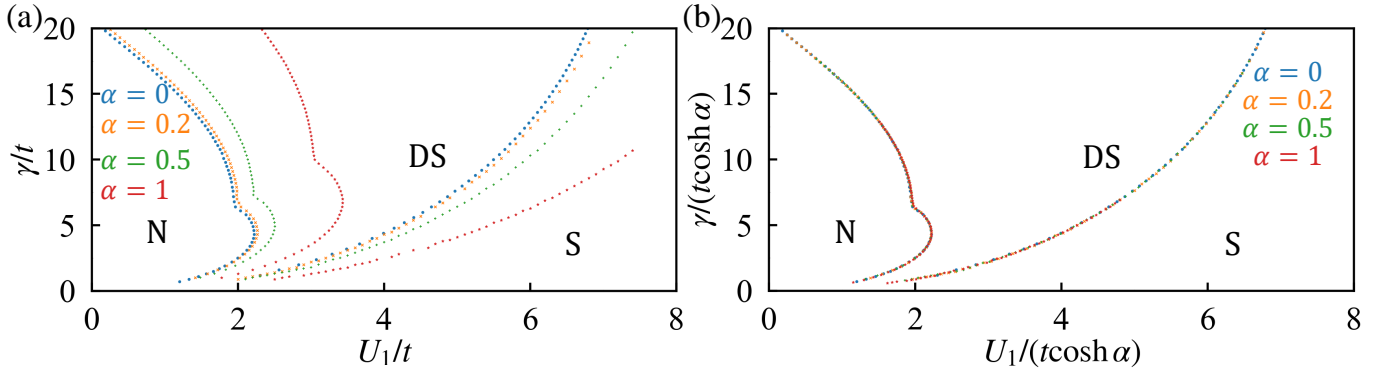


FIG. 7. Phase diagram of the NH BCS model with asymmetric hopping and complex-valued interactions with energy unit (a) t and (b) $t \cosh \alpha$. N denotes the normal state where the gap equation (27) has a trivial solution. The gap equation has a non-trivial solution and $\text{Re}E_{\text{cond}} < 0$ in the superfluid state, which is denoted as S. DS state appears when a non-trivial solution of the NH gap equation exists and $\text{Re}E_{\text{cond}} > 0$. In Fig. 7(a), as increasing α , the phase boundaries shift to the lower right. In Fig. 7(b), By rescaling the energy unit, the phase boundary for different α collapses into the single phase boundary.

our model. For example, if we use $\Omega \sim 2\pi \times 6.3\text{kHz}$ and $t \sim 2\pi \times 0.32\text{kHz}$ given in Refs. [24, 34], the one-body loss rate $\kappa_1 = \Omega^2/(2t\delta) \sim 2\pi \times 3.1 \times 10^2\text{kHz}$ should be required, and the asymmetry of the hopping is given by $\delta = 0.2$ in this case. Third, the implementation of the two-body loss can be done by using the photoassociation [38]. For ^{173}Yb , the two-body loss rate is tunable up to several ms^{-1} [24], which means that $\gamma_2/t \sim 5$ can be reached. Finally, to extract the conditional dynamics where the quantum jump does not occur, we can employ the quantum-trajectory method and obtain the special measurement outcome by using the quantum-gas microscope [43, 100–104]. Although the quantum-gas microscope is available in one- and two-dimensional systems, the NH phase in three-dimensional systems can be observed by focusing on the short time dynamics. Thus, the parameter region of our model can be accessed in the experiment.

Appendix B: The effect of the other type of the asymmetric hopping

Here we consider the other type of the asymmetric hopping on a three-dimensional Hubbard model with a complex-valued interaction. The kinetic term of the NH Hamiltonian is given by

$$H_{\text{kin}} = -t' \sum_{\langle i,j \rangle, \sigma} (e^{\alpha} c_{i,\sigma}^{\dagger} c_{j,\sigma} + e^{-\alpha} c_{j,\sigma}^{\dagger} c_{i,\sigma}), \quad (\text{B1})$$

where the asymmetry of the hopping is α . After the Fourier transformation, the energy dispersion is written as

$$\xi_k = -2t' \cosh \alpha \sum_{j=x,y,z} \cos k_j - 2it' \sinh \alpha \sum_{j=x,y,z} \sin k_j. \quad (\text{B2})$$

Then, the NH BCS Hamiltonian (10), the NH gap equation (27), and the condensation energy (29) are given by replacing ξ_k by that in Eq. (B2). In Fig. 7, we show the phase diagram of the NH BCS model with complex-valued interactions and the asymmetric hopping in Eq. (B1). Here, we discuss how the asymmetric hopping affects the phase diagram. As increasing the asymmetric hopping amplitude α , the phase boundary between the normal and the DS state shifts to the upper right [see the lines for $\alpha = 0.2, 0.5$, and 1.0 in Fig. 7(a)]. The phase boundary between the DS state and the superfluid state also shifts to the lower right in Fig. 7(a). These shifts of the phase boundary indicate that the superfluidity becomes unstable due to the asymmetry of the hopping α . However, the phase boundary with different asymmetric hopping collapses into a single phase boundary [see Fig. 7(b)] by rescaling the energy unit as $t \rightarrow t \cosh \alpha$. To understand that, we first consider the NH gap equation (27). By changing the energy unit, the NH gap equation (27) for $\alpha > 0$ is the same as that for $\alpha = 0$. Thus, the phase diagram for different asymmetry of the hopping α collapses into that for $\alpha = 0$. Such a collapse into a single phase boundary indicates that the superfluid order parameter Δ_0 for $\alpha > 0$, and $(U_1/t, \gamma/t) = (U_0/(t \cosh \alpha), \gamma_0/(t \cosh \alpha))$ is $\cosh \alpha$ times than that for $\alpha = 0$, and $(U_1/t, \gamma/t) = (U_0/t, \gamma_0/t)$. The collapse into a single line of the condensation energy E_{cond} also occurs by performing the same rescaling. We can illustrate the phase diagram for complex-valued interactions with any asymmetric hopping α by changing the energy unit. As increasing α , we rescale the energy unit as a larger one, which indicates that the real and the imaginary part of the order parameter and the condensation energy become small. This corresponds to the instability of the superfluids.

- [2] S. Inouye, M. Andrews, J. Stenger, H.-J. Miesner, D. M. Stamper-Kurn, and W. Ketterle, Observation of Feshbach resonances in a Bose–Einstein condensate, *Nature* **392**, 151 (1998).
- [3] C. Chin, R. Grimm, P. Julienne, and E. Tiesinga, Feshbach resonances in ultracold gases, *Rev. Mod. Phys.* **82**, 1225 (2010).
- [4] R. Zhang, Y. Cheng, H. Zhai, and P. Zhang, Orbital Feshbach Resonance in Alkali-Earth Atoms, *Phys. Rev. Lett.* **115**, 135301 (2015).
- [5] M. Höfer, L. Riegger, F. Scazza, C. Hofrichter, D. R. Fernandes, M. M. Parish, J. Levinsen, I. Bloch, and S. Fölling, Observation of an Orbital Interaction-Induced Feshbach Resonance in ^{173}Yb , *Phys. Rev. Lett.* **115**, 265302 (2015).
- [6] G. Pagano, M. Mancini, G. Cappellini, L. Livì, C. Sias, J. Catani, M. Inguscio, and L. Fallani, Strongly Interacting Gas of Two-Electron Fermions at an Orbital Feshbach Resonance, *Phys. Rev. Lett.* **115**, 265301 (2015).
- [7] G. Cappellini, L. F. Livì, L. Franchi, D. Tusi, D. Benedicto Orenes, M. Inguscio, J. Catani, and L. Fallani, Coherent Manipulation of Orbital Feshbach Molecules of Two-Electron Atoms, *Phys. Rev. X* **9**, 011028 (2019).
- [8] M. W. Zwierlein, C. A. Stan, C. H. Schunck, S. M. F. Raupach, A. J. Kerman, and W. Ketterle, Condensation of Pairs of Fermionic Atoms near a Feshbach Resonance, *Phys. Rev. Lett.* **92**, 120403 (2004).
- [9] C. A. Regal, M. Greiner, and D. S. Jin, Observation of Resonance Condensation of Fermionic Atom Pairs, *Phys. Rev. Lett.* **92**, 040403 (2004).
- [10] C. H. Schunck, Y.-i. Shin, A. Schirotzek, and W. Ketterle, Determination of the fermion pair size in a resonantly interacting superfluid, *Nature* **454**, 739 (2008).
- [11] A. Behrle, T. Harrison, J. Kombe, K. Gao, M. Link, J.-S. Bernier, C. Kollath, and M. Köhl, Higgs mode in a strongly interacting fermionic superfluid, *Nat. Phys.* **14**, 781 (2018).
- [12] H. Biss, L. Sobirey, N. Luick, M. Bohlen, J. J. Kinnunen, G. M. Bruun, T. Lompe, and H. Moritz, Excitation Spectrum and Superfluid Gap of an Ultracold Fermi Gas, *Phys. Rev. Lett.* **128**, 100401 (2022).
- [13] L. Sobirey, H. Biss, N. Luick, M. Bohlen, H. Moritz, and T. Lompe, Observing the Influence of Reduced Dimensionality on Fermionic Superfluids, *Phys. Rev. Lett.* **129**, 083601 (2022).
- [14] M. Holten, L. Bayha, K. Subramanian, S. Brandstetter, C. Heintze, P. Lunt, P. M. Preiss, and S. Jochim, Observation of Cooper pairs in a mesoscopic two-dimensional Fermi gas, *Nature (London)* **606**, 287 (2022).
- [15] J. K. Chin, D. E. Miller, Y. Liu, C. Stan, W. Setiawan, C. Sanner, K. Xu, and W. Ketterle, Evidence for superfluidity of ultracold fermions in an optical lattice, *Nature (London)* **443**, 961 (2006).
- [16] R. Jördens, N. Strohmaier, K. Günter, H. Moritz, and T. Esslinger, A Mott insulator of fermionic atoms in an optical lattice, *Nature (London)* **455**, 204 (2008).
- [17] L. W. Cheuk, M. A. Nichols, K. R. Lawrence, M. Okan, H. Zhang, and M. W. Zwierlein, Observation of 2D Fermionic Mott Insulators of ^{40}K with Single-Site Resolution, *Phys. Rev. Lett.* **116**, 235301 (2016).
- [18] S. Smale, P. He, B. A. Olsen, K. G. Jackson, H. Sharum, S. Trotzky, J. Marino, A. M. Rey, and J. H. Thywissen, Observation of a transition between dynamical phases in a quantum degenerate Fermi gas, *Sci. Adv.* **5**, eaax1568 (2019).
- [19] J. A. Muniz, D. Barberena, R. J. Lewis-Swan, D. J. Young, J. R. Cline, A. M. Rey, and J. K. Thompson, Exploring dynamical phase transitions with cold atoms in an optical cavity, *Nature (London)* **580**, 602 (2020).
- [20] A. J. Daley, Quantum trajectories and open many-body quantum systems, *Adv. Phys.* **63**, 77 (2014).
- [21] L. M. Sieberer, M. Buchhold, and S. Diehl, Keldysh field theory for driven open quantum systems, *Rep. Prog. Phys.* **79**, 096001 (2016).
- [22] Y. Ashida, Z. Gong, and M. Ueda, Non-Hermitian physics, *Adv. Phys.* **69**, 249 (2020).
- [23] V. Meden, L. Grunwald, and D. M. Kennes, \mathcal{PT} -symmetric, non-Hermitian quantum many-body physics—a methodological perspective, *Rep. Prog. Phys.* **86**, 124501 (2023).
- [24] K. Honda, S. Taie, Y. Takasu, N. Nishizawa, M. Nakagawa, and Y. Takahashi, Observation of the Sign Reversal of the Magnetic Correlation in a Driven-Dissipative Fermi Gas in Double Wells, *Phys. Rev. Lett.* **130**, 063001 (2023).
- [25] M.-Z. Huang, J. Mohan, A.-M. Visuri, P. Fabritius, M. Talebi, S. Wili, S. Uchino, T. Giamarchi, and T. Esslinger, Superfluid Signatures in a Dissipative Quantum Point Contact, *Phys. Rev. Lett.* **130**, 200404 (2023).
- [26] G. Barontini, R. Labouvie, F. Stubenrauch, A. Vogler, V. Guarnera, and H. Ott, Controlling the Dynamics of an Open Many-Body Quantum System with Localized Dissipation, *Phys. Rev. Lett.* **110**, 035302 (2013).
- [27] Y. S. Patil, S. Chakram, and M. Vengalattore, Measurement-Induced Localization of an Ultracold Lattice Gas, *Phys. Rev. Lett.* **115**, 140402 (2015).
- [28] R. Labouvie, B. Santra, S. Heun, and H. Ott, Bistability in a Driven-Dissipative Superfluid, *Phys. Rev. Lett.* **116**, 235302 (2016).
- [29] H. P. Lüschen, P. Bordia, S. S. Hodgman, M. Schreiber, S. Sarkar, A. J. Daley, M. H. Fischer, E. Altman, I. Bloch, and U. Schneider, Signatures of Many-Body Localization in a Controlled Open Quantum System, *Phys. Rev. X* **7**, 011034 (2017).
- [30] L. Corman, P. Fabritius, S. Häusler, J. Mohan, L. H. Dogra, D. Husmann, M. Lebrat, and T. Esslinger, Quantized conductance through a dissipative atomic point contact, *Phys. Rev. A* **100**, 053605 (2019).
- [31] Y. Takasu, T. Yagami, Y. Ashida, R. Hamazaki, Y. Kuno, and Y. Takahashi, \mathcal{PT} -symmetric non-Hermitian quantum many-body system using ultracold atoms in an optical lattice with controlled dissipation, *Prog. Theor. Exp. Phys.* **2020**, 12A110 (2020).
- [32] R. Bouganne, M. Bosch Aguilera, A. Ghermaoui, J. Beugnon, and F. Gerbier, Anomalous decay of coherence in a dissipative many-body system, *Nat. Phys.* **16**, 21 (2020).
- [33] J. Benary, C. Baals, E. Bernhart, J. Jiang, M. Röhrle, and H. Ott, Experimental observation of a dissipative phase transition in a multi-mode many-body quantum system, *New Journal of Physics* **24**, 103034 (2022).
- [34] Z. Ren, D. Liu, E. Zhao, C. He, K. K. Pak, J. Li, and G.-B. Jo, Chiral control of quantum states in non-Hermitian spin-orbit-coupled fermions, *Nat. Phys.* **18**, 385 (2022).
- [35] N. Syassen, D. M. Bauer, M. Lettner, T. Volz, D. Dietze, J. J. García-Ripoll, J. I. Cirac, G. Rempe, and S. Dürr, Strong Dissipation Inhibits Losses and Induces Correlations in Cold Molecular Gases, *Science* **320**, 1329 (2008).
- [36] B. Yan, S. A. Moses, B. Gadway, J. P. Covey, K. R. Hazzard, A. M. Rey, D. S. Jin, and J. Ye, Observation of dipolar spin-exchange interactions with lattice-confined polar molecules, *Nature (London)* **501**, 521 (2013).
- [37] B. Zhu, B. Gadway, M. Foss-Feig, J. Schachenmayer, M. L. Wall, K. R. A. Hazzard, B. Yan, S. A. Moses, J. P. Covey, D. S. Jin, J. Ye, M. Holland, and A. M. Rey, Suppressing the Loss

- of Ultracold Molecules Via the Continuous Quantum Zeno Effect, *Phys. Rev. Lett.* **112**, 070404 (2014).
- [38] T. Tomita, S. Nakajima, I. Danshita, Y. Takasu, and Y. Takahashi, Observation of the Mott insulator to superfluid crossover of a driven-dissipative Bose-Hubbard system, *Sci. Adv.* **3**, e1701513 (2017).
- [39] K. Sponselee, L. Freystatzky, B. Abeln, M. Diem, B. Hundt, A. Kochanke, T. Ponath, B. Santra, L. Mathey, K. Sengstock, and C. Becker, Dynamics of ultracold quantum gases in the dissipative Fermi-Hubbard model, *Quantum Sci. Technol.* **4**, 014002 (2018).
- [40] T. Tomita, S. Nakajima, Y. Takasu, and Y. Takahashi, Dissipative Bose-Hubbard system with intrinsic two-body loss, *Phys. Rev. A* **99**, 031601 (2019).
- [41] M. J. Mark, E. Haller, K. Lauber, J. G. Danzl, A. Janisch, H. P. Büchler, A. J. Daley, and H.-C. Nägerl, Preparation and Spectroscopy of a Metastable Mott-Insulator State with Attractive Interactions, *Phys. Rev. Lett.* **108**, 215302 (2012).
- [42] M. J. Mark, S. Flannigan, F. Meinert, J. P. D’Incao, A. J. Daley, and H.-C. Nägerl, Interplay between coherent and dissipative dynamics of bosonic doublons in an optical lattice, *Phys. Rev. Res.* **2**, 043050 (2020).
- [43] Y. Ashida, S. Furukawa, and M. Ueda, Quantum critical behavior influenced by measurement backaction in ultracold gases, *Phys. Rev. A* **94**, 053615 (2016).
- [44] Y. Ashida, S. Furukawa, and M. Ueda, Parity-time-symmetric quantum critical phenomena, *Nat. Commun.* **8**, 15791 (2017).
- [45] J. A. S. Lourenço, R. L. Eneias, and R. G. Pereira, Kondo effect in a \mathcal{PT} -symmetric non-Hermitian Hamiltonian, *Phys. Rev. B* **98**, 085126 (2018).
- [46] M. Nakagawa, N. Kawakami, and M. Ueda, Non-Hermitian Kondo Effect in Ultracold Alkaline-Earth Atoms, *Phys. Rev. Lett.* **121**, 203001 (2018).
- [47] R. Hanai, A. Edelman, Y. Ohashi, and P. B. Littlewood, Non-Hermitian Phase Transition from a Polariton Bose-Einstein Condensate to a Photon Laser, *Phys. Rev. Lett.* **122**, 185301 (2019).
- [48] R. Hamazaki, K. Kawabata, and M. Ueda, Non-Hermitian Many-Body Localization, *Phys. Rev. Lett.* **123**, 090603 (2019).
- [49] M. Nakagawa, N. Tsuji, N. Kawakami, and M. Ueda, Dynamical Sign Reversal of Magnetic Correlations in Dissipative Hubbard Models, *Phys. Rev. Lett.* **124**, 147203 (2020).
- [50] K. Yamamoto, Y. Ashida, and N. Kawakami, Rectification in nonequilibrium steady states of open many-body systems, *Phys. Rev. Res.* **2**, 043343 (2020).
- [51] T. Liu, J. J. He, T. Yoshida, Z.-L. Xiang, and F. Nori, Non-Hermitian topological Mott insulators in one-dimensional fermionic superlattices, *Phys. Rev. B* **102**, 235151 (2020).
- [52] Z. Xu and S. Chen, Topological Bose-Mott insulators in one-dimensional non-Hermitian superlattices, *Phys. Rev. B* **102**, 035153 (2020).
- [53] S. Mu, C. H. Lee, L. Li, and J. Gong, Emergent Fermi surface in a many-body non-Hermitian fermionic chain, *Phys. Rev. B* **102**, 081115 (2020).
- [54] D.-W. Zhang, Y.-L. Chen, G.-Q. Zhang, L.-J. Lang, Z. Li, and S.-L. Zhu, Skin superfluid, topological Mott insulators, and asymmetric dynamics in an interacting non-Hermitian Aubry-André-Harper model, *Phys. Rev. B* **101**, 235150 (2020).
- [55] R. Hanai and P. B. Littlewood, Critical fluctuations at a many-body exceptional point, *Phys. Rev. Res.* **2**, 033018 (2020).
- [56] N. Matsumoto, K. Kawabata, Y. Ashida, S. Furukawa, and M. Ueda, Continuous Phase Transition without Gap Closing in Non-Hermitian Quantum Many-Body Systems, *Phys. Rev. Lett.* **125**, 260601 (2020).
- [57] K. Yang, S. C. Morampudi, and E. J. Bergholtz, Exceptional Spin Liquids from Couplings to the Environment, *Phys. Rev. Lett.* **126**, 077201 (2021).
- [58] X. Z. Zhang and Z. Song, η -pairing ground states in the non-Hermitian Hubbard model, *Phys. Rev. B* **103**, 235153 (2021).
- [59] M. Nakagawa, N. Kawakami, and M. Ueda, Exact Liouvillian Spectrum of a One-Dimensional Dissipative Hubbard Model, *Phys. Rev. Lett.* **126**, 110404 (2021).
- [60] H. Tajima and K. Iida, Non-Hermitian Ferromagnetism in an Ultracold Fermi Gas, *Journal of the Physical Society of Japan* **90**, 024004 (2021).
- [61] K. Yamamoto, M. Nakagawa, M. Tezuka, M. Ueda, and N. Kawakami, Universal properties of dissipative Tomonaga-Luttinger liquids: Case study of a non-Hermitian XXZ spin chain, *Phys. Rev. B* **105**, 205125 (2022).
- [62] S.-B. Zhang, M. M. Denner, T. c. v. Bzdušek, M. A. Sentef, and T. Neupert, Symmetry breaking and spectral structure of the interacting Hatano-Nelson model, *Phys. Rev. B* **106**, L121102 (2022).
- [63] B. Dóra and C. P. Moca, Full counting statistics in the many-body Hatano-Nelson model, *Phys. Rev. B* **106**, 235125 (2022).
- [64] T. Orito and K.-I. Imura, Entanglement dynamics in the many-body Hatano-Nelson model, *Phys. Rev. B* **108**, 214308 (2023).
- [65] K. Yamamoto and N. Kawakami, Universal description of dissipative Tomonaga-Luttinger liquids with $SU(N)$ spin symmetry: Exact spectrum and critical exponents, *Phys. Rev. B* **107**, 045110 (2023).
- [66] S. E. Han, D. J. Schultz, and Y. B. Kim, Complex fixed points of the non-Hermitian Kondo model in a Luttinger liquid, *Phys. Rev. B* **107**, 235153 (2023).
- [67] C. Wang, T.-C. Yi, J. Li, and R. Mondaini, Non-Hermitian Haldane-Hubbard model: Effective description of one- and two-body dissipation, *Phys. Rev. B* **108**, 085134 (2023).
- [68] L. Rosso, A. Biella, J. De Nardis, and L. Mazza, Dynamical theory for one-dimensional fermions with strong two-body losses: Universal non-Hermitian Zeno physics and spin-charge separation, *Phys. Rev. A* **107**, 013303 (2023).
- [69] R. Sarkar, A. Bandyopadhyay, and A. Narayan, Non-Hermiticity induced exceptional points and skin effect in the Haldane model on a dice lattice, *Phys. Rev. B* **107**, 035403 (2023).
- [70] X.-J. Yu, Z. Pan, L. Xu, and Z.-X. Li, Non-Hermitian Strongly Interacting Dirac Fermions, *Phys. Rev. Lett.* **132**, 116503 (2024).
- [71] L. Yang, Dissipative-interaction-induced polaron-molecule transition in three-dimensional Fermi polarons, *Phys. Rev. A* **109**, 063305 (2024).
- [72] K. Yamamoto, M. Nakagawa, and N. Kawakami, Correlation versus Dissipation in a Non-Hermitian Anderson Impurity Model, *arXiv:2408.03494*.
- [73] Y.-J. Han, Y.-H. Chan, W. Yi, A. J. Daley, S. Diehl, P. Zoller, and L.-M. Duan, Stabilization of the p -Wave Superfluid State in an Optical Lattice, *Phys. Rev. Lett.* **103**, 070404 (2009).
- [74] S. Diehl, W. Yi, A. J. Daley, and P. Zoller, Dissipation-Induced d -Wave Pairing of Fermionic Atoms in an Optical Lattice, *Phys. Rev. Lett.* **105**, 227001 (2010).
- [75] A. Ghatak and T. Das, Theory of superconductivity with non-Hermitian and parity-time reversal symmetric Cooper pairing symmetry, *Phys. Rev. B* **97**, 014512 (2018).
- [76] K. Yamamoto, M. Nakagawa, K. Adachi, K. Takasan, M. Ueda, and N. Kawakami, Theory of Non-Hermitian Fermionic Superfluidity with a Complex-Valued Interaction, *Phys. Rev. Lett.* **123**, 123601 (2019).

- [77] F. m. c. Damanet, E. Mascarenhas, D. Pekker, and A. J. Daley, Controlling Quantum Transport via Dissipation Engineering, *Phys. Rev. Lett.* **123**, 180402 (2019).
- [78] K. Yamamoto, M. Nakagawa, N. Tsuji, M. Ueda, and N. Kawakami, Collective Excitations and Nonequilibrium Phase Transition in Dissipative Fermionic Superfluids, *Phys. Rev. Lett.* **127**, 055301 (2021).
- [79] P. He, H.-T. Ding, and S.-L. Zhu, Geometry and superfluidity of the flat band in a non-Hermitian optical lattice, *Phys. Rev. A* **103**, 043329 (2021).
- [80] T. Kanazawa, Non-Hermitian BCS-BEC crossover of Dirac fermions, *J. High Energy Phys.* **03** (2021), 121.
- [81] M. Iskin, Non-Hermitian BCS-BEC evolution with a complex scattering length, *Phys. Rev. A* **103**, 013724 (2021).
- [82] H. Li, X.-H. Yu, M. Nakagawa, and M. Ueda, Yang-Lee Zeros, Semicircle Theorem, and Nonunitary Criticality in Bardeen-Cooper-Schrieffer Superconductivity, *Phys. Rev. Lett.* **131**, 216001 (2023).
- [83] H. Tajima, Y. Sekino, D. Inotani, A. Dohi, S. Nagataki, and T. Hayata, Non-Hermitian topological Fermi superfluid near the p -wave unitary limit, *Phys. Rev. A* **107**, 033331 (2023).
- [84] G. Mazza and M. Schirò, Dissipative dynamics of a fermionic superfluid with two-body losses, *Phys. Rev. A* **107**, L051301 (2023).
- [85] S. Takemori, K. Yamamoto, and A. Koga, Theory of non-Hermitian fermionic superfluidity on a honeycomb lattice: Interplay between exceptional manifolds and Van Hove singularity, *Phys. Rev. B* **109**, L060501 (2024).
- [86] H. Tajima, Y. Sekino, D. Inotani, A. Dohi, S. Nagataki, and T. Hayata, Non-Hermitian p -wave superfluid and effects of the inelastic three-body loss in a one-dimensional spin-polarized Fermi gas, *Phys. Rev. Res.* **6**, 023060 (2024).
- [87] T. Shi, S. Wang, Z. Zheng, and W. Zhang, Two-dimensional non-Hermitian fermionic superfluidity with spin imbalance, *Phys. Rev. A* **109**, 063306 (2024).
- [88] T. Fukui and N. Kawakami, Breakdown of the Mott insulator: Exact solution of an asymmetric Hubbard model, *Phys. Rev. B* **58**, 16051 (1998).
- [89] N. Hatano and D. R. Nelson, Localization Transitions in Non-Hermitian Quantum Mechanics, *Phys. Rev. Lett.* **77**, 570 (1996).
- [90] N. Hatano and D. R. Nelson, Vortex pinning and non-Hermitian quantum mechanics, *Phys. Rev. B* **56**, 8651 (1997).
- [91] N. Hatano and D. R. Nelson, Non-Hermitian delocalization and eigenfunctions, *Phys. Rev. B* **58**, 8384 (1998).
- [92] Z. Gong, Y. Ashida, K. Kawabata, K. Takasan, S. Higashikawa, and M. Ueda, Topological Phases of Non-Hermitian Systems, *Phys. Rev. X* **8**, 031079 (2018).
- [93] F. Reiter and A. S. Sørensen, Effective operator formalism for open quantum systems, *Phys. Rev. A* **85**, 032111 (2012).
- [94] T. Liu, Y.-R. Zhang, Q. Ai, Z. Gong, K. Kawabata, M. Ueda, and F. Nori, Second-Order Topological Phases in Non-Hermitian Systems, *Phys. Rev. Lett.* **122**, 076801 (2019).
- [95] A. M. Clogston, Upper Limit for the Critical Field in Hard Superconductors, *Phys. Rev. Lett.* **9**, 266 (1962).
- [96] B. S. Chandrasekhar, A NOTE ON THE MAXIMUM CRITICAL FIELD OF HIGH-FIELD SUPERCONDUCTORS, *Applied Physics Letters* **1**, 7 (1962).
- [97] D. E. Sheehy and L. Radzihovsky, BEC-BCS crossover, phase transitions and phase separation in polarized resonantly-paired superfluids, *Annals of Physics* **322**, 1790 (2007).
- [98] E. Müller-Hartmann, Correlated fermions on a lattice in high dimensions, *Zeitschrift für Physik B Condensed Matter* **74**, 507 (1989).
- [99] W. Metzner and D. Vollhardt, Correlated Lattice Fermions in $d = \infty$ Dimensions, *Phys. Rev. Lett.* **62**, 324 (1989).
- [100] H. Ott, Single atom detection in ultracold quantum gases: a review of current progress, *Rep. Prog. Phys.* **79**, 054401 (2016).
- [101] D. Mitra, P. T. Brown, E. Guardado-Sanchez, S. S. Kondov, T. Devakul, D. A. Huse, P. Schauß, and W. S. Bakr, Quantum gas microscopy of an attractive Fermi-Hubbard system, *Nat. Phys.* **14**, 173 (2018).
- [102] P. T. Brown, E. Guardado-Sanchez, B. M. Spar, E. W. Huang, T. P. Devereaux, and W. S. Bakr, Angle-resolved photoemission spectroscopy of a Fermi-Hubbard system, *Nat. Phys.* **16**, 26 (2020).
- [103] C. F. Chan, M. Gall, N. Wurz, and M. Köhl, Pair correlations in the attractive Hubbard model, *Phys. Rev. Res.* **2**, 023210 (2020).
- [104] T. Hartke, B. Oreg, C. Turnbaugh, N. Jia, and M. Zwierlein, Direct observation of nonlocal fermion pairing in an attractive Fermi-Hubbard gas, *Science* **381**, 82 (2023).
- [105] K. Kawabata, K. Shiozaki, M. Ueda, and M. Sato, Symmetry and topology in non-Hermitian physics, *Physical Review X* **9**, 041015 (2019).
- [106] K. Kawabata, K. Shiozaki, and S. Ryu, Many-body topology of non-Hermitian systems, *Phys. Rev. B* **105**, 165137 (2022).
- [107] Y. Fuji and Y. Ashida, Measurement-induced quantum criticality under continuous monitoring, *Phys. Rev. B* **102**, 054302 (2020).
- [108] S. Goto and I. Danshita, Measurement-induced transitions of the entanglement scaling law in ultracold gases with controllable dissipation, *Phys. Rev. A* **102**, 033316 (2020).
- [109] Q. Tang and W. Zhu, Measurement-induced phase transition: A case study in the nonintegrable model by density-matrix renormalization group calculations, *Phys. Rev. Res.* **2**, 013022 (2020).
- [110] S.-K. Jian, C. Liu, X. Chen, B. Swingle, and P. Zhang, Measurement-Induced Phase Transition in the Monitored Sachdev-Ye-Kitaev Model, *Phys. Rev. Lett.* **127**, 140601 (2021).
- [111] M. Block, Y. Bao, S. Choi, E. Altman, and N. Y. Yao, Measurement-Induced Transition in Long-Range Interacting Quantum Circuits, *Phys. Rev. Lett.* **128**, 010604 (2022).
- [112] T. Minato, K. Sugimoto, T. Kuwahara, and K. Saito, Fate of Measurement-Induced Phase Transition in Long-Range Interactions, *Phys. Rev. Lett.* **128**, 010603 (2022).
- [113] E. V. H. Doggen, Y. Gefen, I. V. Gornyi, A. D. Mirlin, and D. G. Polyakov, Generalized quantum measurements with matrix product states: Entanglement phase transition and clusterization, *Phys. Rev. Res.* **4**, 023146 (2022).
- [114] K. Yamamoto and R. Hamazaki, Localization properties in disordered quantum many-body dynamics under continuous measurement, *Phys. Rev. B* **107**, L220201 (2023).
- [115] L. Zhou, Entanglement phase transitions in non-Hermitian quasicrystals, *Phys. Rev. B* **109**, 024204 (2024).
- [116] T. Tsuno, S. Taie, Y. Takasu, K. Yamashita, T. Ozawa, and Y. Takahashi, Gain engineering and topological atom laser in synthetic dimensions, *arXiv:2404.13769*.